Inorganic Chemistry

Article

pubs.acs.org/IC

Sandwich-Type Mixed Tetrapyrrole Rare-Earth Triple-Decker Compounds. Effect of the Coordination Geometry on the Single-Molecule-Magnet Nature

Jinglan Kan,[†] Hailong Wang,[†] Wei Sun,[†] Wei Cao,[†] Jun Tao,[‡] and Jianzhuang Jiang*,[†]

[†]Beijing Key Laboratory for Science and Application of Functional Molecular and Crystalline Materials, Department of Chemistry, University of Science and Technology Beijing, Beijing, China

[‡]State Key Laboratory of Physical Chemistry of Solid Surfaces and Department of Chemistry, College of Chemistry and Chemical Engineering, Xiamen University, Xiamen, China

Supporting Information

ABSTRACT: Employment of the raise-by-one step method starting from M(TClPP)(acac) (acac = monoanion of acetylacetone) and [Pc(OPh)$_8$]-M′[Pc(OPh)$_8$] led to the isolation and free modulation of the two rare-earth ions in the series of four mixed tetrapyrrole dysprosium sandwich complexes {(TClPP)M[Pc(OPh)$_8$]M′[Pc(OPh)$_8$]} [**1**−**4**; TClPP = dianion of *meso*-tetrakis(4-chlorophenyl)porphyrin; Pc(OPh)$_8$ = dianion of 2,3,9,10,16,17,23,24-octa(phenoxyl)phthalocyanine; M−M′ = Dy−Dy, Y−Dy, Dy−Y, and Y−Y]. Single-crystal X-ray diffraction analysis reveals different octacoordination geometries for the two metal ions in terms of the twist angle (defined as the rotation angle of one coordination square away from the eclipsed conformation with the other) between the two neighboring tetrapyrrole rings for the three dysprosium-containing isostructural triple-decker compounds, with the metal ion locating between an inner phthalocyanine ligand and an outer porphyrin ligand with a twist angle of 9.64−9.90° and the one between two phthalocyanine ligands of 25.12−25.30°. Systematic and comparative studies over the magnetic properties reveal magnetic-field-induced single-molecule magnet (SMM), SMM, and non-SMM nature for **1**−**3**, respectively, indicating the dominant effect of the coordination geometry of the spin carrier, instead of the f−f interaction, on the magnetic properties. The present result will be helpful for the future design and synthesis of tetrapyrrole lanthanide SMMs with sandwich molecular structures.

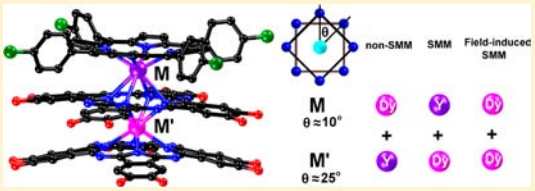

INTRODUCTION

Both lanthanide- and transition-metal-based single-molecule magnets (SMMs) have attracted increasing research interest because of their potential applications in magnetic storage and molecular spintronics associated with the magnetic bistability.[1] Investigations clearly revealed the relationship of the energy barrier in reversing magnetization for most polynuclear transition-metal-based SMMs with the magnetic anisotropy projected on the ground exchange and the multiplet projection of the total spin on the symmetry axis due to the much larger exchange coupling than the zero-field-splitting effect on an individual metal.[2] In good contrast, origination of the height of the barrier in reversing magnetization for lanthanide-based analogues was only proposed to be associated with the larger zero-field-splitting effect on the spin carrier and/or the weak interionic exchange interaction.[3] Limited studies conducted thus far suggest the magnetic exchange interaction on the SMM behavior of the lanthanide-based complexes without concerning the contribution from the coordination geometry of an individual lanthanide ion and vice versa.[4] Obviously, suitable polylanthanide SMM systems that allow studies toward clarifying the contribution of the coordination geometry and/or f−f magnetic interaction are highly desired. The availability of sandwich-type multinuclear rare-earth complexes with mixed tetrapyrrole rings provides a good chance to work for this target owing to the inherent advantage in modulating the rare-earth ions and tuning the coordination geometry for lanthanide ions and f−f magnetic interaction.[5] In the present paper, a series of four sandwich-type mixed (phthalocyaninato)(porphyrinato) di-rare-earth complexes with isostructural triple-decker molecular structure {(TClPP)M[Pc(OPh)$_8$]M′[Pc(OPh)$_8$]} (**1**−**4**; M−M′ = Dy−Dy, Y−Dy, Dy−Y, and Y−Y) have been designed, synthesized, and structurally characterized [TClPP = dianion of 5,10,15,20-tetrakis(4-chlorophenyl)porphyrin and Pc(OPh)$_8$ = dianion of 2,3,9,10,16,17,23,24-octa(phenoxyl)-phthalocyanine] (Scheme 1). Free modulation in the two shortly separated rare-earth ions between dysprosium and yttrium in combination with their different octacoordination geometries (in terms of the twist angle defined as the rotation angle of one coordination square from tetrapyrrole away from the eclipsed conformation with the other) renders it possible toward clarifying the effect of the coordination geometry of the spin carrier and/or the f−f interaction on their magnetic properties. Systematic and comparative studies over the magnetic properties revealed magnetic-field-induced SMM,

Received: February 24, 2013
Published: July 11, 2013

   dx.doi.org/10.1021/ic400485y | *Inorg. Chem.* 2013, 52, 8505−8510

Scheme 1. Synthesis of the Sandwich-Type Mixed (Phthalocyaninato)(porphyrinato) Di-Rare-Earth Triple-Decker Complexes with M−M′ = Dy−Dy, Y−Dy, Dy−Y, and Y−Y for 1−4

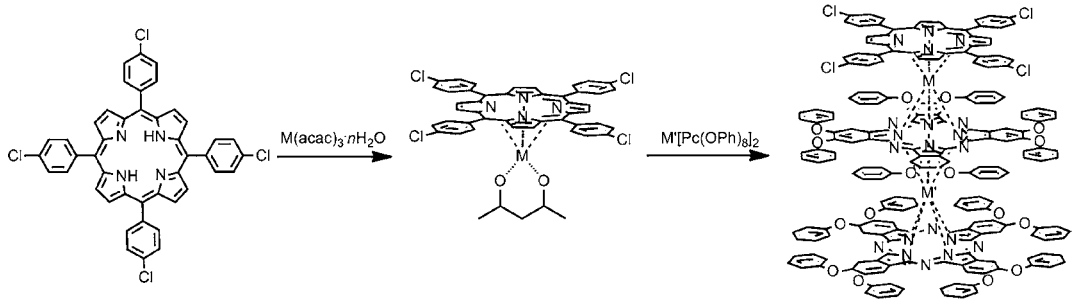

SMM, and non-SMM nature for the Dy−Dy, Y−Dy, and Dy−Y systems, respectively, indicating the dominant effect of the coordination geometry of the spin carrier, instead of the f−f interaction, on the magnetic properties of the sandwich-type tetrapyrrole lanthanide triple-decker systems.

RESULTS AND DISCUSSION

Treatment of the half-sandwich porphyrinato rare-earth complex M(TClPP)(acac), generated in situ from the reaction between $[M(acac)_3]\cdot nH_2O$ (acac = monoanion of acetylacetone) and H_2TClPP, with bis(phthalocyaninato) rare-earth complex $[Pc(OPh)_8]M'[Pc(OPh)_8]$ in refluxing 1,2,4-trichlorobenzene (TCB) for 4 h led to isolation of the sandwich-type mixed (phthalocyaninato)(porphyrinato) di-rare-earth complexes **1**−**3**.[6] For the purpose of a comparative study, **4** was also obtained with the half-sandwich porphyrinatoyttrium complex and the bis(phthalocyaninato)yttrium double-decker compound as starting materials. It is worth noting that employment of such a kind of raise-by-one step synthesis method allows free modulation on the two rare-earth species between dysprosium and yttrium in the triple-decker structure. In addition to elemental analysis, these four triple-decker compounds have also been characterized by a series of spectroscopic methods including matrix-assisted laser desorption ionization time-of-flight (MALDI-TOF) mass and NMR spectroscopy (Figure 1 and Figures S1−S6 and Table S1 in the Supporting Information). The MALDI-TOF mass spectra of these four compounds clearly showed intense signals for molecular ion $[M + H]^+$ (Figure S1 in the Supporting Information). As is clearly shown in Figure S2 in the Supporting Information and summarized in Table S1 in the Supporting Information, the two singlet signals at δ 9.44 and 8.50 in the diyttrium triple-decker compound **4** are attributed to the nonperipheral protons of the $Pc^{in}(OPh)_8$ and $Pc^{out}(OPh)_8$ rings, respectively. Replacement of one of the two diamagnetic yttrium ions by a paramagnetic dysprosium ion leads to an obvious upfield shift of the nonperipheral proton signals of the $Pc^{in}(OPh)_8$ and $Pc^{out}(OPh)_8$ rings to δ −44.65 and −38.97 for **2** as well as δ −4.42 and 12.14 for **3** (Figures S4 and S5 in the Supporting Information), revealing the long-distance lanthanide-induced shift of the dysprosium(III) ion to the whole triple-decker molecular skeleton.[7] A further change in the remaining diamagnetic yttrium ion in **2** and **3** to a paramagnetic dysprosium ion in **1** induces a further shift of the nonperipheral proton signals of the $Pc^{in}(OPh)_8$ and $Pc^{out}(OPh)_8$ rings to δ −59.66 and −35.58 (Figures 1 and S3 in the Supporting Information), suggesting the presence of f−f interaction between the two shortly separated dysprosium ions in this didysprosium triple-decker compound **1**.[7]

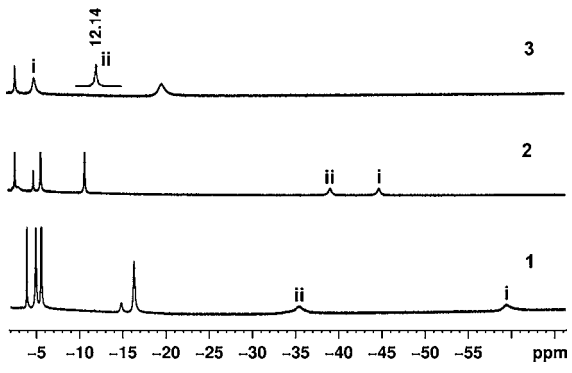

Figure 1. ^{1}H NMR spectra for triple-decker complexes **1**−**3** in $CDCl_3$, showing the singals of the nonperipheral protons of the $Pc^{in}(OPh)_8$ (i) and $Pc^{out}(OPh)_8$ (ii) rings.

The mixed tetrapyrrole nature with sandwich-type triple-decker molecular structures for **1**−**3** was clearly revealed by single-crystal X-ray diffraction analysis. Single crystals of all of the three triple-decker compounds suitable for X-ray diffraction analysis were obtained by diffusion of methanol onto the solution of a corresponding compound in chloroform. The isostructural compounds crystallize in the tetragonal system with the space group *P*4*nc*, and each unit cell contains two sandwich-type triple-decker molecules of **1**−**3** (Table S2 in the Supporting Information). The structural data of **1**−**3** are summarized in Table S3 in the Supporting Information. As shown in Figure 2A,B, the outer phthalocyanine and porphyrin ligands are connected by two rare-earth ions sharing a common phthalocyanine ligand, forming the isostructural triple-decker molecular structure for **1**. This is also true for the analogous triple-decker complexes **2** and **3** (Figures S7 and S8 in the Supporting Information). The two rare-earth ions M and M′ in these three compounds are separated by a short distance of 3.586(3)−3.605(3) Å, leading to magnetic−dipolar interaction.[5f,8] The rare-earth ion sandwiched between the inner phthalocyanine and outer porphyrin ligands adopts a more distorted square-antiprism (SAP) geometry comprised of four isoindole nitrogen atoms of the phthalocyanine ligand and four pyrrole nitrogen atoms of the porphyrin ligand with a twist angle ϕ_1 of 9.64−9.90°, and the other between two phthalocyanine ligands employs a distorted SAP octacoordination geometry constructed from eight isoindole nitrogen atoms with a twist angle ϕ_2 of 25.12−25.30° (Figure 2C).

To evaluate the effect of the coordination geometry around the dysprosium ion and the f−f interaction between the two dysprosium ions in the didysprosium triple-decker compound

dx.doi.org/10.1021/ic400485y | Inorg. Chem. 2013, 52, 8505−8510

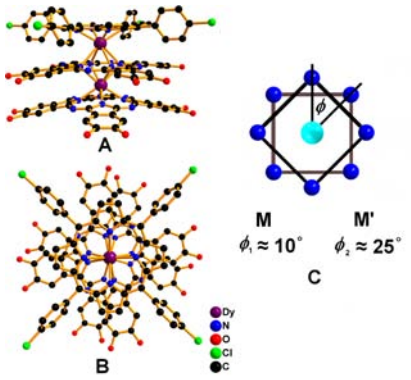

Figure 2. Molecular structure of **1** in a side view (A) and a top view (B), with all of the hydrogen atoms, benzene rings of phenoxy groups, and solvent molecules omitted for clarity. The twist angles ϕ_1 and ϕ_2 are defined as the twist angles around M and M′ for **1**−**3**, respectively (C).

on the magnetic properties, the static magnetic properties of the whole series of three complexes **1**−**3** have been systematically and comparatively investigated. As can be seen in Figure S2 in the Supporting Information, the curve of the magnetic susceptibility $\chi_M T$ for **1**−**3** shows a temperature-dependent character. The $\chi_M T$ value of 28.09 cm^3 K mol^{-1} for **1** at 300 K is consistent with the value of 28.34 cm^3 K mol^{-1} for two dysprosium(III) ions [$^6H_{15/2}$, $S = {}^5/_2$, $L = 5$, $g = {}^4/_3$], while those of 14.77 and 14.32 cm^3 K mol^{-1} for **2** and **3** are consistent with the expected value of 14.17 cm^3 K mol^{-1} for one dysprosium(III) ion.[9] When the temperature is lowered, the $\chi_M T$ values of these three compounds decrease slowly until about 15 K, then decreasing to minimum values of 15.06, 8.84, and 7.69 cm^3 K mol^{-1} for **1**−**3** at 2 K, respectively. The overall magnetic behavior of all of these three compounds can be attributed mainly to the crystal-field effects such as thermal depopulation of the dysprosium(III) Stark sublevels and intramolecular magnetic interaction.[9b−d] Actually, the intramolecular Dy−Dy interaction in **1** could be analyzed in a qualitative manner according to the $\Delta\chi_M T$ tendency by subtracting the $\chi_M T$ values of the monodysprosium triple-decker compounds **2** and **3** from that of **1**.[9d] As shown in Figure 3, the increase of $\Delta\chi_M T$ for **1** following a decrease of the temperature indicates the ferromagnetic interaction between the two dysprosium(III) ions in this compound.[9d] In addition, as shown in Figure S9 in the Supporting Information, the three nonsuperposition curves for **1**−**3** display a rapid increase at low field and eventually achieve the maximum value of 12.40−12.61 μ_B for the former triple-decker compound and 5.48−7.61 μ_B for the latter two compounds at 5 T without reaching the theoretical magnetization saturation [20.00 and 10.00 μ_B for two and one dysprosium(III) ($^6H_{15/2}$, $S = {}^5/_2$, $L = 5$, $g = {}^4/_3$) ions, respectively], revealing the crystal-field effect on the dysprosium ion.[9b−d] As also can be seen in this figure, the nonsuperposition field-dependent magnetization curves obtained at 2.0, 3.0, and 5.0 K for the di- and monodysprosium involved triple-decker compounds **1**−**3** indicate the presence of crystal-field effects, thus leading to magnetic anisotropy for the dysprosium(III) ion in these triple-decker complexes.

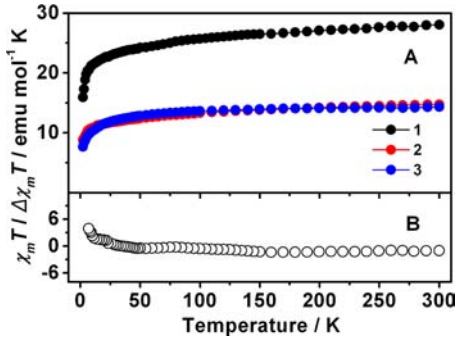

Figure 3. Temperature dependence of $\chi_M T$ for **1**−**3** (A) as well as that of $\Delta\chi_M T = [\chi_M(\mathbf{1}) - \chi_M(\mathbf{2}) - \chi_M(\mathbf{3})]T$ (B).

Figure 4 shows the temperature dependence of the alternating-current (ac) magnetic susceptibility of **1**−**3** under a zero direct-current (dc) magnetic field oscillating at 10−997 Hz. As can be seen, only monodysprosium triple-decker compound **2** with a conformation of {(TClPP)Y[Pc(OPh)$_8$]-Dy[Pc(OPh)$_8$]} exhibits a frequency-dependent character in the in-phase (χ') and out-of-phase (χ'') signals, indicating the slow relaxation of magnetization and revealing the SMM nature for this complex. However, the relaxation time of magnetization cannot be deduced for this compound most probably because of the location of the relaxation mode at higher frequency than 997 Hz associated with the fast quantum tunneling. In contrast, the other monodysprosium triple-decker compound **3** with a conformation of {(TClPP)Dy[Pc(OPh)$_8$]Y[Pc(OPh)$_8$]} does not show a frequency-dependent character in the in-phase (χ') and out-of-phase (χ'') signals (Figure 4), revealing its non-

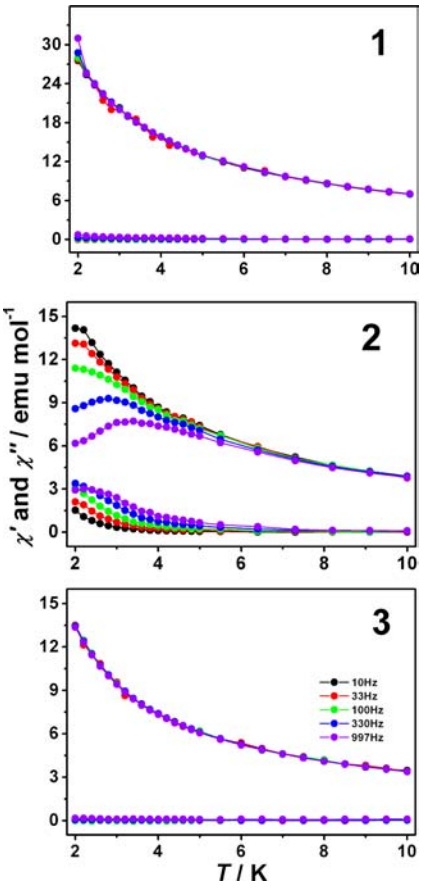

Figure 4. Plots for the temperature dependence of the in-phase (χ') and out-of-phase (χ'') ac susceptibilities of **1**−**3** under a zero applied dc magnetic field.

dx.doi.org/10.1021/ic400485y | Inorg. Chem. 2013, 52, 8505−8510

SMM nature under a zero applied dc magnetic field. Unexpectedly, this is also true for the didysprosium triple-decker compound **1** despite involvement of the same $[Pc(OPh)_8]Dy[Pc(OPh)_8]\}$ fragment as that in analogous **2** (Figure 4). Anyway, these results suggest the more significant effect of the coordination geometry of a lanthanide ion relative to the magnetic interaction between the lanthanide ions on the magnetic properties of sandwich-type tetrapyrrole rare-earth triple-decker complexes.

For the purpose of further understanding the magnetic behavior of these sandwich-type tetrapyrrole dysprosium triple-decker complexes, dynamic magnetic measurements over **1**−**3** have been conducted under an external dc, 2000 Oe magnetic field. As expected, the frequency-dependent character in the in-phase (χ') and out-of-phase (χ'') signals still exists for **2** (Figure 5), confirming the SMM nature of this compound. In addition,

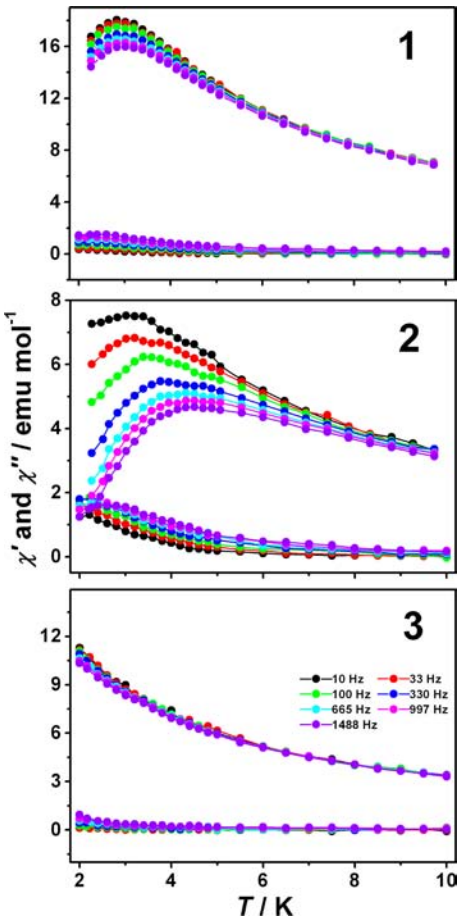

Figure 5. Plots for the temperature dependence of the in-phase (χ') and out-of-phase (χ'') ac susceptibilities of **1**−**3** under a 2000 Oe applied dc magnetic field.

the peak of the out-of-phase signal (χ'') for this compound could be observed until a frequency as low as 330 Hz, indicating the effective suppression of quantum tunneling of magnetization (QTM) under an external dc, 2000 Oe magnetic field. On the basis of a thermally activated mechanism, $\tau = \tau_0 \exp(U_{eff}/kT)$ and $\tau = 1/2\pi\nu$, the Arrhenius law fitting for the data under a 2000 Oe magnetic field was carried out. As shown in Figure S10 in the Supporting Information, a linear relationship exists between $\ln(\tau)$ and $1/T$ in the temperature range of 2.26−2.80 K for **2**, which, in turn, results in a barrier U_{eff} = 17.3 cm^{-1} (24.9 K) and $\tau_0 = 1.52 \times 10^{-7}$ s with R = 0.9989, suggesting the presence of one thermally activated relaxation process.[9d] Not surprisingly, typical slow relaxation of magnetization behavior could still not be observed for the other monodysprosium **3** involving $(TClPP)Dy[Pc(OPh)_8]$ instead of the $[Pc(OPh)_8]Dy[Pc(OPh)_8]$ fragment. However, under an external dc, 2000 Oe magnetic field, the didysprosium triple-decker compound **1** starts to show a frequency-dependent character in the in-phase (χ') and out-of-phase (χ'') signals in the whole oscillating range of 10−1488 Hz employed, indicating the field-induced SMM nature of this compound.[10]

Comparative inspection over the magnetic properties in association with the detailed molecular conformations of **1**−**3** seems to reveal the significant role of the bis(phthalocyaninato)dysprosium fragment $[Pc(OPh)_8]Dy[Pc(OPh)_8]$ over the (phthalocyaninato)(porphyrinato)dysprosium fragment $(TClPP)Dy[Pc(OPh)_8]$ in a triple-decker molecule in contributing to the SMM nature of the mixed tetrapyrrole rare-earth complexes most probably because of the less significant deviation of the coordination geometry of the dysprosium ion sandwiched between two phthalocyanine ligands, in comparison with the one between one porphyrin and one phthalocyanine ligands, from the SAP in terms of the twist angle between two tetrapyrrole rings, as detailed above. This appears in line with that derived from previous studies over the magnetic properties of sandwich-type tetrapyrrole dysprosium compounds with double-, triple-, and quadruple-decker molecular structures to the point that the degree of suppression of the QTM was revealed to increase along with a decrease in the deviation of the twist angle from 45° despite the typical slow relaxation of magnetization behavior, as revealed for all of the thus-far-reported tetrapyrrole dysprosium sandwich complexes with the twist angle between two tetrapyrrole rings ranging from 18 to 43°.[8,9c,d,11] Nevertheless, the non-SMM nature revealed for the triple-decker compound **3** with $(TClPP)Dy[Pc(OPh)_8]$ as the sole spin-carrier fragment, in which the twist angle between two tetrapyrrole rings amounts to less than 10°, actually 9.68°, appears to give an obvious hint for the future design and synthesis of tetrapyrrole dysprosium SMMs with sandwich molecular structure. Additional support for this point comes from the non-SMM character of the didysprosium triple-decker compound **1** under a zero applied dc magnetic field despite involvement of the better spin-carrier fragment $[Pc(OPh)_8]Dy[Pc(OPh)_8]\}$ in addition to $(TClPP)Dy[Pc(OPh)_8]$.

CONCLUSIONS

In conclusion, three sandwich-type mixed tetrapyrrole di-rare-earth complexes with dysprosium as spin carrier(s) and an isostructural triple-decker conformation have been designed and synthesized. Free modulation in the two shortly separated rare-earth ions between dysprosium and yttrium in combination with their different octacoordination geometry in terms of the twist angle for the dysprosium ion between the two neighboring tetrapyrrole rings in the triple-decker molecule renders it possible toward clarifying the effect of the coordination geometry of the spin carrier and/or the f−f interaction on the magnetic properties for these sandwich systems. The magnetic-field-induced SMM, SMM, and non-SMM nature revealed for the Dy−Dy, Y−Dy, and Dy−Y systems, respectively, indicate the dominant effect of the coordination geometry of the spin carrier, instead of the f−f interaction, on the magnetic properties.

dx.doi.org/10.1021/ic400485y | Inorg. Chem. 2013, 52, 8505−8510

EXPERIMENTAL SECTION

Measurements. ^{1}H, ^{1}H−^{1}H COSY, and ^{13}C NMR spectra were recorded on a Bruker DPX 400 spectrometer in $CDCl_3$. Spectra were referenced internally using the residual solvent resonance (δ 7.26 for ^{1}H NMR) relative to $SiMe_4$. Electronic absorption spectra were recorded with a Hitachi U-4100 spectrophotometer. MALDI-TOF mass spectra were taken on a Bruker BIFLEX III ultrahigh-resolution Fourier transform ion cyclotron resonance (FT-ICR) mass spectrometer with α-cyano-4-hydroxycinnamic acid as the matrix. Elemental analysis was performed on an Elementar Vario El III.

Chemicals. All reagents and solvents were used as received. The compounds of $M(acac)_3{\cdot}H_2O$ (M = Dy and Y)[12] and H_2TClPP[13] and the homoleptic bis(phthalocyaninato) rare-earth(III) complexes $M'[Pc(OPh)_8]_2$ [$Pc(OPh)_8$ = 2,3,9,10,16,17,23,24-octaphenoxyphthalocyaninate][14] were prepared according to literature methods.

General Procedure for the Synthesis of {(TClPP)M[Pc(OPh)$_8$]-M′[Pc(OPh)$_8$]} (1−4; M−M′ = Dy−Dy, Y−Dy, Dy−Y, and Y−Y). A mixture of H_2(TClPP) (0.03 mmol) and $[M(acac)_3]{\cdot}nH_2O$ (ca. 0.04 mmol) in TCB (2 mL) was refluxed for 4 h under a slow stream of nitrogen. The resulting dark-cherry-red solution was cooled, then $M'[Pc(OPh)_8]_2$ (0.02 mmol) was added, and the mixture was refluxed for a further 4 h. After cooling to room temperature, 10 mL of *n*-hexane was added to the mixture. The precipitate was filtered off and washed with *n*-hexane and methanol. The residue left was chromatographed on a silica gel column with CH_2Cl_2 as the eluent. Repeated chromatography followed by recrystallization from $CHCl_3$ and methanol gave pure compound as a dark powder. In a similar manner, **4** was also isolated. Single crystals of **1**−**3** suitable for X-ray diffraction analysis were obtained by diffusion of methanol onto a solution of the corresponding compound in chloroform.

{(TClPP)Dy[Pc(OPh)$_8$]Dy[Pc(OPh)$_8$]} ***(1)***. Yield: ca. 36 mg (50%). UV−vis [$CHCl_3$; λ_{max}, nm (log(ε), M^{-1} cm^{-1})]: 364 (5.30), 412 (5.16), 625 (4.91), 752 (4.58). ^{1}H NMR (400 MHz, $CDCl_3$, δ): 34.66 (s, Por-Ph-*H*), 12.46 (s, Por-Ph-*H*), 3.21 (s, Por-Ph-*H*), 1.74 (s, Pc^{out}-Ph-H_p), 1.21 (s, Pc^{out}-Ph-H_m), −4.27 (s, Pc^{out}-Ph-H_o), −5.28 (s, Pc^{in}-Ph-H_p), −5.90 (s, Pc^{in}-Ph-H_m), −15.03 (s, Por-Ph-*H*), −16.48 (s, Pc^{in}-Ph-H_o), −35.58 (s, Pc^{out}-H_α), −59.66 (s, Pc^{in}-H_α). MALDI-TOF MS: an isotopic cluster peaking at *m*/*z* 3575.5. Calcd for $C_{204}H_{120}Cl_4Dy_2N_{20}O_{16}$: *m*/*z* 3575.1 ([M + H]$^+$). Anal. Calcd for $C_{204}H_{120}Cl_4Dy_2N_{20}O_{16}$: C, 68.55; H, 3.38; N, 7.84. Found: C, 68.76; H, 3.46; N, 7.73.

{(TClPP)Y[Pc(OPh)$_8$]Dy[Pc(OPh)$_8$]} ***(2)***. Yield: ca. 30 mg (43%). UV−vis [$CHCl_3$; λ_{max}, nm (log(ε), M^{-1} cm^{-1})]: 364 (5.22), 410 (5.08), 625 (4.83), 752 (4.47). ^{1}H NMR (400 MHz, $CDCl_3$, δ): 31.73 (s, Por-Ph-*H*), 28.01 (s, Por-Ph-*H*), 14.95 (s, Por-Ph-*H*), 1.62 (s, Pc^{out}-Ph-H_m), 2.07 (s, Pc^{out}-Ph-H_p), −0.99 (s, Pc^{in}-Ph-H_p), −2.23 (s, Pc^{in}-Ph-H_m), −4.39 (s, Por-Ph-*H*), −5.25 (s, Pc^{out}-Ph-H_o), −10.38 (s, Pc^{in}-Ph-H_o), −38.97 (s, Pc^{out}-H_α), −44.65 (s, Pc^{in}-H_α). MALDI-TOF MS: an isotopic cluster peaking at *m*/*z* 3501.9. Calcd for $C_{204}H_{120}Cl_4DyN_{20}O_{16}Y$: *m*/*z* 3501.5 ([M + H]$^+$). Anal. Calcd for $C_{204}H_{120}Cl_4Y_2N_{20}O_{16}$: C, 70.00; H, 3.46; N, 8.00. Found: C, 70.07; H, 3.41; N, 7.89.

{(TClPP)Dy[Pc(OPh)$_8$]Y[Pc(OPh)$_8$]} ***(3)***. Yield: ca. 52 mg (75%). UV−vis [$CHCl_3$; λ_{max}, nm (log(ε), M^{-1} cm^{-1})]: 362 (5.20), 412 (5.06), 625 (4.82), 753 (4.50). ^{1}H NMR (400 MHz, $CDCl_3$, δ): 12.14 (s, Pc^{out}-H_α), 8.56 (s, Por-Ph-*H*), 7.26 (s, Pc^{out}-Ph-H_p), 7.03 (s, Pc^{out}-Ph-H_m), 6.89 (s, Pc^{out}-Ph-H_o), 4.76 (s, Por-Ph-*H*), 4.75 (s, Pc^{in}-Ph-H_p), 4.57 (s, Pc^{in}-Ph-H_m), 2.33 (s, Pc^{in}-Ph-H_o), −2.23 (s, Por-H_β), −4.42 (s, Pc^{in}-H_α), −19.33 (s, Por-Ph-*H*). MALDI-TOF MS: an isotopic cluster peaking at *m*/*z* 3502.0. Calcd for $C_{204}H_{120}Cl_4DyN_{20}O_{16}Y$: *m*/*z* 3501.5 ([M + H]$^+$). Anal. Calcd for $C_{204}H_{120}Cl_4Dy_2N_{20}O_{16}$: C, 70.00; H, 3.46; N, 8.00. Found: C, 70.28; H, 3.40; N, 7.93.

{(TClPP)Y[Pc(OPh)$_8$]Y[Pc(OPh)$_8$]} ***(4)***. Yield: ca. 40 mg (58%). UV−vis [$CHCl_3$; λ_{max}, nm (log(ε), M^{-1} cm^{-1})]: 362 (5.18), 412 (5.03), 625 (4.80), 754 (4.46). ^{1}H NMR (400 MHz, $CDCl_3$, δ): 9.44−9.46 (d, 4H, Por-Ph-*H*), 9.44 (s, 8H, Pc^{in}-H_α), 8.50 (s, 8H, Pc^{out}-H_α), 7.73−7.77 (d, 16H, Pc^{in}-Ph-H_o), 7.61−7.63 (m, 24H, Pc^{in}-Ph-H_p and Pc^{in}-Ph-H_m), 7.35−7.39 (s, Pc^{out}-Ph-H_o), 7.31−7.31 (d, 4H, Por-Ph-*H*), 7.25 (Por-H_β), 7.12−7.18 (m, 28H, Por-Ph-*H*, Pc^{out}-Ph-H_p and Pc^{out}-Ph-H_m), 6.32−6.34 (d, 4H, Por-Ph-*H*). ^{13}C NMR (400 MHz, $CDCl_3$, δ): 157.87, 156.69, 156.57, 154.20, 152.34, 149.89, 148.98, 140.08, 133.68, 133.51, 132.96, 132.73, 132.53, 130.74, 129.94, 127.77, 127.16, 126.24, 124.97, 123.23, 120.29, 119.93, 117.50, 114.69, 112.59. MALDI-TOF MS: an isotopic cluster peaking at *m*/*z* 3429.1. Calcd for $C_{204}H_{120}Cl_4N_{20}O_{16}Y_2$: *m*/*z* 3427.9 ([M + H]$^+$). Anal. Calcd for $C_{204}H_{120}Cl_4N_{20}O_{16}Y_2$: C, 71.50; H, 3.53; N, 8.17. Found: C, 71.40; H, 3.49; N, 7.99.

X-ray Crystallographic Analysis of 1−3. Single crystals suitable for X-ray diffraction analysis were grown by diffusing MeOH into the $CHCl_3$ solutions of these compounds. The details of the structure refinement are given in Table S2 in the Supporting Information, and structural data of **1**−**3** are summarized in Table S3 in the Supporting Information. Crystal data for **1**−**3** were determined by X-ray diffraction analysis at 100−126 K using an Oxford Diffraction Gemini E system with Cu Kα radiation (λ = 1.5418 Å), using a ω scan mode with an increment of 1°. The preliminary unit cell parameters were obtained from 30 frames. The final unit cell parameters were obtained by global refinement of reflections obtained from integration of all of the frame data. The collected frames were integrated using the preliminary cell-orientation matrix. *SMART* software was used for data collection and processing, *ABSpack* for absorption correction,[15] and *SHELXL* for space group and structure determination, refinement, graphics, and structure reporting.[16] CCDC 902562−902564 for **1**−**3**, respectively, containing the supplementary crystallographic data for this paper can be obtained free of charge from the Cambridge Crystallographic Data Centre via www.ccdc.cam.ac.uk/data_request/cif.

ASSOCIATED CONTENT

Supporting Information

MS and ^{1}H NMR spectra for **1**−**4**, ^{1}H−^{1}H COSY NMR spectra for **2**−**4**, ^{13}C NMR spectrum of **4**, $\chi_M T$ and $\Delta\chi_M T$, *M* vs *H*/*T*, ln(τ) vs 1/*T* for **2**, NMR data and assignments for **1**−**4**, details of the structure refinement and structural data of **1**−**3**, and CIF file of **1**−**3**. This material is available free of charge via the Internet at http://pubs.acs.org.

AUTHOR INFORMATION

Corresponding Author

*E-mail: jianzhuang@ustb.edu.cn.

Notes

The authors declare no competing financial interest.

ACKNOWLEDGMENTS

Financial support from the National Key Basic Research Program of China (Grants 2013CB933402 and 2012CB224801), Natural Science Foundation of China, Beijing Municipal Commission of Education, and State Key Laboratory of Physical Chemistry of Solid Surfaces is gratefully acknowledged.

REFERENCES

(1) (a) Gatteschi, D.; Sessoli, R. *Angew. Chem., Int. Ed.* **2003**, *42*, 268. (b) Gatteschi, D.; Sessoli, R.; Villain, J. *Molecular Nanomagnets*; Oxford University Press: Oxford, U.K., 2006. (c) Bogani, L.; Wernsdorfer, W. *Nat. Mater.* **2008**, *7*, 179.

(2) Gatteschi, D.; Fittipaldi, M.; Sangregorio, C.; Sorace, L. *Angew. Chem., Int. Ed.* **2012**, *51*, 4792.

(3) (a) Westin, L. G.; Kritikos, M.; Caneschi, A. *Chem. Commun.* **2003**, 1012. (b) Zaleski, C. M.; Depperman, E. C.; Kampf, J. W.; Kirk, M. L.; Pecoraro, V. L. *Angew. Chem., Int. Ed.* **2004**, *43*, 3912. (c) Ishikawa, N.; Sugita, M.; Wernsdorfer, W. *J. Am. Chem. Soc.* **2005**, *127*, 3650.

(4) Mironov, V. S.; Chibotaru, L. F.; Ceulemans, A. *J. Am. Chem. Soc.* **2003**, *125*, 9750.
(5) (a) Ng, D. K. P.; Jiang, J. *Chem. Soc. Rev.* **1997**, *26*, 433. (b) Buchler, J.; Ng, D. K. P. *The Porphyrin Handbook*; Kadish, K. M., Smith, K. M., Guilard, R., Ed.; Academic Press: New York, 2000; pp 245−290. (c) Jiang, J.; Kasuga, K.; Arnold, D. P. *Supramolecular Photo-Sensitive and Electroactive Materials*; Nalwa, H. S., Ed.; Academic Press: New York, 2001; pp 113−210. (d) Jiang, J.; Bao, M.; Rintoul, L.; Arnold, D. P. *Coord. Chem. Rev.* **2006**, *250*, 424. (e) Jiang, J.; Ng, D. K. P. *Acc. Chem. Res.* **2009**, *42*, 79. (f) Lu, J.; Zhang, D.; Wang, H.; Jiang, J.; Zhang, X. *Inorg. Chem. Commun.* **2010**, *13*, 1144. (g) Sakaue, S.; Fuyuhiro, A.; Fukuda, T.; Ishikawa, N. *Chem. Commun.* **2012**, *48*, 5337.
(6) (a) Jiang, J.; Bian, Y.; Furuya, F.; Liu, W.; Choi, M. T. M.; Kobayashi, N.; Li, H.-W.; Yang, Q.; Mak, T. C. W.; Ng, D. K. P. *Chem.—Eur. J.* **2001**, *7*, 5059. (b) Sun, X.; Li, R.; Wang, D.; Dou, J.; Zhu, P.; Lu, F.; Ma, C.; Choi, C.-F.; Cheng, D. Y. Y.; Ng, D. K. P.; Kobayashi, N.; Jiang, J. *Eur. J. Inorg. Chem.* **2004**, 3806. (c) Wang, R.; Li, R.; Bian, Y.; Choi, C.-F.; Ng, D. K. P.; Dou, J.; Wang, D.; Zhu, P.; Ma, C.; Hartnell, R. D.; Arnold, D. P.; Jiang, J. *Chem.—Eur. J.* **2005**, *11*, 7351. (d) Zhu, P.; Pan, N.; Li, R.; Dou, J.; Zhang, Y.; Cheng, D. Y. Y.; Wang, D.; Ng, D. K. P.; Jiang, J. *Chem.—Eur. J.* **2005**, *11*, 1425. (e) Sheng, N.; Li, R.; Choi, C.-F.; Su, W.; Ng, D. K. P.; Cui, X.; Yoshida, K.; Kobayashi, N.; Jiang, J. *Inorg. Chem.* **2006**, *45*, 3794. (f) Jiang, J. Functional Phthalocyanine Molecular Materials. In *Structure and Bonding*; Mingos, D. M. P., Ed.; Springer-Verlag: Heidelberg, Germany, 2010; Vol. *135*. (g) Wang, H.; Wang, K.; Bian, Y.; Jiang, J.; Kobayashi, N. *Chem. Commun.* **2011**, *47*, 6879. (h) Wang, H.; Kobayashi, N.; Jiang, J. *Chem.—Eur. J.* **2012**, *18*, 1047.
(7) (a) Ishikawa, N.; Iino, T.; Kaizu, Y. *J. Phys. Chem. A* **2003**, *107*, 7879. (b) Birin, K. P.; Gorbunova, Y. G.; Tsivadze, A. Yu. *Dalton Trans.* **2012**, *41*, 9672. (c) Wang, H.; Liu, T.; Wang, K.; Duan, C.; Jiang, J. *Chem.—Eur. J.* **2012**, *18*, 7691.
(8) Katoh, K.; Horii, Y.; Yasuda, N.; Wernsdorfer, W.; Toriumi, K.; Breedlove, B. K.; Yamashita, M. *Dalton Trans.* **2012**, *41*, 13582.
(9) (a) Zheng, Y.-Z.; Lan, Y.; Wernsdorfer, W.; Anson, C. E.; Powell, A. K. *Chem.—Eur. J.* **2009**, *15*, 12566. (b) Jiang, S.-D.; Wang, B.-W.; Su, G.; Wang, Z.-M.; Gao, S. *Angew. Chem., Int. Ed.* **2010**, *49*, 7448. (c) Wang, H.; Qian, K.; Wang, K.; Bian, Y.; Jiang, J.; Gao, S. *Chem. Commun.* **2011**, *47*, 9624. (d) Wang, H.; Wang, K.; Tao, J.; Jiang, J. *Chem. Commun.* **2012**, *48*, 2973.
(10) Koo, B. H.; Lim, K. S.; Ryu, D. W.; Lee, W. R.; Koh, E. K.; Hong, C. S. *Chem. Commun.* **2012**, *48*, 2519.
(11) (a) Koike, N.; Uekusa, H.; Ohashi, Y.; Harnoode, C.; Kitamura, F.; Ohsaka, T.; Tokuda, K. *Inorg. Chem.* **1996**, *35*, 5798. (b) Ishikawa, N.; Sugita, M.; Okubo, T.; Tanaka, N.; Iino, T.; Kaizu, Y. *Inorg. Chem.* **2003**, *42*, 2440. (c) Keiichi, K.; Kaori, U.; Brian, K.; Masahiro, Y. *Sci. China: Chem.* **2012**, *55*, 918.
(12) Hu, B.-Y.; Yuan, Y.-J.; Xiao, J.; Guo, C.-C.; Liu, Q.; Tan, Z.; Li, Q.-H. *J. Porphyrins Phthalocyanines* **2008**, *12*, 27.
(13) Stites, J. G.; McCarty, C. N.; Quill, L. L. *J. Am. Chem. Soc.* **1948**, *70*, 3142.
(14) Lu, G.; Bai, M.; Li, R.; Zhang, X.; Ma, C.; Lo, P.-C.; Ng, D. K. P.; Jiang, J. *Eur. J. Inorg. Chem.* **2006**, 3703.
(15) Blessing, R. H. *Acta Crystallogr.* **1995**, *A51*, 33−38.
(16) *SHELXL Reference Manual*, version 5.1; Bruker Analytical X-Ray Systems: Madison, WI, 1997.